

## PAPR Reduction of OFDM Signals using Gradual Projection Active Constellation Extension and Sequential Block Grouping Tone Reservation Hybrid Scheme

Eugen-Victor Cuteanu

Communication Department  
Politehnica University, Faculty of Electronics and  
Telecommunications  
Timisoara, Romania  
victor.cuteanu@gmail.com

Alexandru Isar

Communication Department  
Politehnica University, Faculty of Electronics and  
Telecommunications  
Timisoara, Romania  
alexandru.isar@etc.upt.ro

**Abstract**—The Orthogonal Frequency Division Multiplexing is one of the widely used modulation techniques in the present broadband wireless technology. The opportunities and challenges of this modulation technique are derived from its native advantages and disadvantages. One of the main problems is the high peak-to-average power ratio of transmission signal due to the superposition of many subcarriers. In previous works, various hybrid peak-to-average power ratio reduction techniques were presented. One of these techniques was the combination of the standard active constellation extension with the sequential tone reservation scheme. This paper presents a new hybrid peak-to-average power ratio reduction technique, which combines other active constellation extension and tone reservation schemes. This is the case of already known smart gradient projection and new proposed signal compression gradual projection active constellation extension and sequential block ordered tone reservation scheme respectively. The simulations shown that the proposed technique realizes an increased peak-to-average power ratio reduction compared to component methods with similar parameters.

**Keywords**-OFDM; PAPR; Gradual Projection; Active Constellation Extension; Sequential Block Grouping; Tone Reservation

### I. INTRODUCTION

The Orthogonal Frequency Division Multiplexing (OFDM) is one of the most efficient and popular modulation techniques used in broadband wireless communication systems like Worldwide Interoperability for Microwave Access (WiMAX), Terrestrial Digital Video Broadcast (DVB-T), or wireline systems like Asymmetric Digital Subscriber Line (ADSL). One of the main practical issues of the OFDM is the Peak-to-Average Power Ratio (PAPR) of the transmitted signal. This high PAPR occurs because of the time-domain superposition of the many data subcarriers which compose the OFDM signal. Due to the large number of subcarriers, the resulting time-domain signal exhibits Rayleigh-like characteristics and large time-domain amplitude variations. These large signal peaks require the high power amplifiers (HPA) to support wide linear dynamic range.

Higher signal level causes non-linear distortions leading to an inefficient operation of HPA, causing intermodulation products resulting unwanted out-of-band power. In order to reduce the PAPR of OFDM signals, many solutions have been proposed and analyzed. For an enhanced PAPR reduction, hybrid techniques were proposed [1]-[6] as well. The efficiency of these methods can be evaluated considering their characteristics of non-linearity, amount of processing and size of side information needed to be sent to receiver.

The class of linear methods is represented by approaches like selective mapping (SLM) [7], Partial Transmit Sequence (PTS) [8], and Tone Reservation (TR) [9].

The SLM method generates several signal replicas based on a set of predefined phase patterns. The algorithm performs vector rotations of each subcarrier from the original frequency domain OFDM signal. For each obtained signal variant, the corresponding PAPR is evaluated. The variant with the lowest PAPR is chosen for the transmission. A similar approach is applied in case of PTS method, where the same rotating phase is applied to a group of subcarriers.

Both methods provide a variable efficiency of PAPR reduction, being dependent by the considered number of angles and phase patterns. An important disadvantage of these methods is that an extended set of different phase patterns leads to an increased computation complexity. To overcome this problem, additional information can be sent to the receiver, in order to reduce its required search space. This approach presents another disadvantage due to reduced payload of each OFDM frame.

Optimizations of these methods have been proposed in several works [10][11].

Another PAPR reduction method is TR, which uses a set of reserved set of subcarriers (tones) to generate signals with lower PAPR level. Besides the advantage of no additional distortion, this method also does not need to transmit additional information to the receiver. Because not all subcarriers are used to transmit useful information, this method is considered to lower the data rate of the OFDM-based systems.

Since the development of the original TR method, in order to reduce the computation complexity and to improve

the performance, several derivate techniques have been proposed: selective mapping of partial tones (SMOPT) [12], One-Tone One-Peak (OTOP) [13] and one-by-one iteration [14].

Another optimized variant of this method proposes to generate tones for the  $K$  largest peaks of the signal. The phases of these tones are chosen to be opposite to  $\varphi_j + n\pi/2$ , where  $\varphi_j$  is the phase of the identified peaks,  $j=1, 2, \dots, K$  and  $n=0, 1, 2, 3$ . The procedure is iterated until convergence reaches the expected threshold [9].

The class of non-linear methods is represented by approaches like active constellation extension (ACE), clipping, partial clipping, and signal compression.

The ACE method change the original OFDM signal by modifying amplitude and phase of tones whose base band modulation symbol is an outer point of the constellation. Those outer signaling points of the conventional constellation are dynamically moved toward outside of the original constellation in order to obtain signal derivatives with reduced PAPR level for the transmitter. The domain for allowed alternative points is chosen so that the signal processing does not reduce the constellation's minimum-distance but lowers the PAPR level [15][16].

For additional PAPR reduction, some proposed derivate methods consider outers points projection onto squares or circles around all the QAM constellation points and intentional distortion within the allowed bounds. The tradeoff between level of the constellation distortion and PAPR level is analyzed and optimized as well [17].

The clipping method is another well known non-linear PAPR reduction technique, where the amplitude of the signal is limited to a given threshold. Because interpolation may generate peak regrowth, different filtering techniques have been proposed. Filtering can also cause peak regrowth, but less than the clipping before interpolation [18].

Another clipping technique supposes that only subcarriers having the highest phase difference between the original signal and its clipped variant will be changed. This is the case of the partial clipping (PC) method [19].

Other group of nonlinear methods is represented by signal companding, originally developed for audio signal compression. These methods are implemented as a digital nonlinear attenuator, which operates at the transmitter before the HPA device.

Some works proposed  $\mu$ -law or A-law companding functions [20] or exponential companding function [21]. In order to reduce the computation complexity, other companding method uses transfer functions split in linear sub-domains with different coefficients. This is the case of the piecewise-scales method [22]. In order to decrease the computation complexity without using sub-domains, other methods consider polynomial ratio functions [23].

At the receiver, the inverse function for signal expanding is applied. This is implemented as a nonlinear amplifier which performs the reverse operation over the time-domain signal. Therefore the nonlinearity does not alter the signal reconstruction process, but has an important impact over the received noise from the communication channel. Therefore the BER performance is strongly impacted by the obtained noise after the signal expanding block.

For an optimized balance between PAPR reduction level and BER degradation, other methods consider adaptive quasi-nonlinear sigmoid transfer functions [6].

For additional PAPR reduction, different hybrid techniques were proposed as well. Their efficiency depends by the characteristics and types of the component methods.

Combinations of a linear method with a non-linear method present better PAPR reduction with moderate increase of computation complexity, and average BER degradation [2][3]. Also, combination of two linear methods, one operating on the data subcarriers and the other one operating on the non-data subcarriers, presents improved efficiency of PAPR reduction [4].

An important characteristic of these combinations is that their computation complexity depends by the cumulative set of parameters describing the total amount of operations required by the component methods.

Additional to previous work [1], the present paper considers as ACE derivatives, the well known smart gradient projection (SGP) method and proposes the signal compression based gradual projection (CGP) method. Also the present paper, proposes a new TR derivate based on the sequential block grouping (SBG) method.

The rest of the paper is organized as follows. The second section describes the proposed hybrid PAPR reduction scheme, when various ACE and TR derivatives are applied. In the third section is described the clipping method as PAPR reduction method of reference. Next, in the forth section, the simulation results for various ACE-TR combinations, highlighted by the computer simulation, are presented and discussed. The PAPR reduction efficiency is evaluated when the new gradual projection ACE and the new sequential block grouping TR schemes are applied. Based on the obtained results, some conclusions are presented in the fifth section.

## II. THE HYBRID METHOD

The proposed hybrid PAPR reduction technique is obtained by serialization of a gradual projection active constellation extension method and sequential tone reservation method.

The main idea for combining the two methods is relying on the observation that the cumulative signal processing for PAPR reduction will increase the overall performance. Furthermore, the idea is based on the fact that each of the considered methods is based on a different principle. One performs a controlled signal distortion and the other realizes different changes of the non-data subcarriers [1].

The block diagram of the proposed method is presented in Figure 1. The performance of the proposed PAPR reduction technique is analyzed with a MATLAB simulator as presented in Figure 2. For this purpose, within this simulator, the samples from the uniformly distributed random generated signal are mapped from binary representation to the M-QAM or M-PSK constellation points. The obtained complex values are grouped in blocks of  $N$  elements each, forming the OFDM symbols.

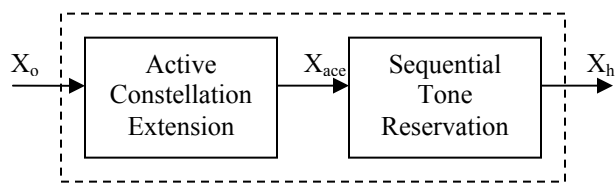


Figure 1. The Hybrid ACE-TR scheme for PAPR reduction.

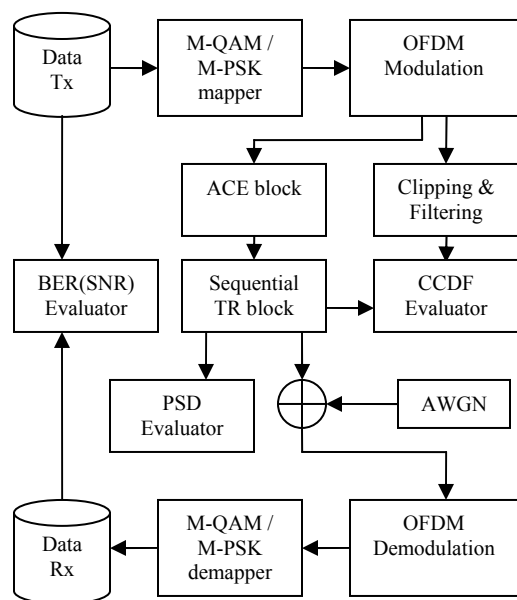


Figure 2. MATLAB model for the analysis of the hybrid PAPR reduction technique.

The obtained OFDM frames are applied to the PAPR reduction blocks. This signal is applied to the Complementary Cumulative Distribution Function (CCDF) block for the evaluation of the PAPR reduction. Next, the resulted signal is applied to the communication channel represented by the complex additive white Gaussian noise. This channel is composed by two independent random Gaussian generated sequences, representing the real and imaginary components of the complex additive noise.

Next, the samples of the noised signal are applied to the demodulator block and M-QAM or M-PSK demapper. Based on the comparison of the obtained received data samples with the initial generated samples, the bit error rate (BER) performance is evaluated.

For a better performance comparison, besides the proposed ACE-TR method, additionally the clipping method [18] is taken into consideration. The PAPR reduction blocks alter the original signal. Due to this fact, for evaluation of communication's performance and efficiency, besides the CCDF and BER characteristics, the simulator estimates the power spectral density (PSD) for the signal obtained after processing for PAPR reduction.

The expression of the PAPR for a given OFDM signal block is given by:

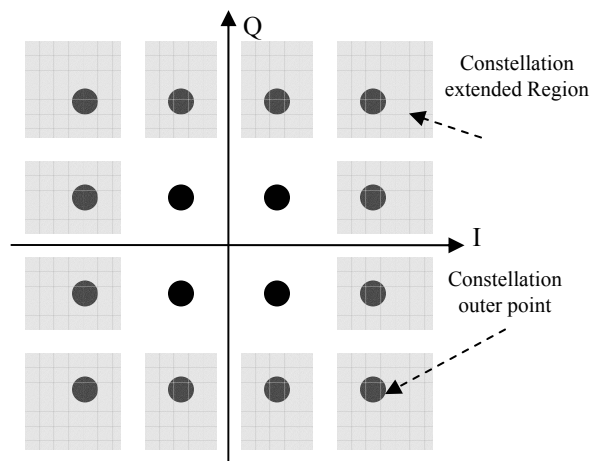


Figure 3. Example of an extended constellation. The original points and allowed extended domain for outer points for 16-QAM are indicated.

$$PAPR(x) = \frac{\max\left\{x(t)^2\right\}}{E\left[x(t)^2\right]}, \quad (1)$$

where  $E[.]$  denotes the expectation operator. This is usually evaluated using the complementary cumulative distribution function (CCDF) of the PAPR:

$$CCDF(Y) = \Pr(PAPR > Y) = 1 - \Pr(PAPR < Y) \quad (2)$$

where  $Y$  is a PAPR threshold.

Within the next paragraphs, the considered ACE and TR methods are described.

#### A. The ACE method

The ACE method requires both time-domain and frequency-domain signal processing. As already mentioned, the main idea of this method is to shift the outer constellation points toward exterior of original constellation generating an alternative representation of the same symbol. The allowed domains for these outer points are presented in Figure 3, when 16-QAM is used as digital modulation.

The boundaries of these domains are constrained by the constellation's minimum-distance. The reason for this limitation is to prevent a decrease of BER performance at the receiver.

In the previous work [1], the considered ACE method was implemented with the projection onto convex sets (POCS) scheme, where ACE constraints are applied after clipping, according with the algorithm presented in [15].

In the preset work, two more ACE derivate methods are considered: one is the SGP-ACE and the other one is the new CGP-ACE proposed method. These methods perform gradual projection, as described in the next paragraphs.

The SGP-ACE method uses a gradient-projection approach, where only a part of the clipping difference is applied to the original time-domain signal. At each iteration,

the ACE constraints are applied in order to ensure that only allowable extension vectors are changed [15].

The implementation of this ACE method requires the following steps:

- 1) Get an OFDM frame with  $N$  subcarriers, represented by the frequency-domain signal  $X_o$ .
- 2) Compute the corresponding time-domain signal  $x[n]$ , by use of IFFT function.
- 3) Search the sample with the maximal amplitude  $x_{max}$  and its index  $n_{max}$ :

$$x_{max} = x[n_{max}]. \quad (3)$$

- 4) Evaluate the average signal amplitude  $x_{mean}$ .
- 5) Define the clipping threshold  $x_{thr}$ , according with the given clipping rate  $CR$ :

$$x_{thr} = x_{max} / CR. \quad (4)$$

- 6) Perform the clipping on the original signal, using the similar relations as in previous algorithm presented. Therefore the new obtained signal satisfies the following condition:

$$\tilde{x}[n] \leq x_{thr} \quad \forall n \in [1, N]. \quad (5)$$

- 7) Compute its corresponding frequency-domain representation:

$$\tilde{X} = FFT(\tilde{x}). \quad (6)$$

- 8) Enforce the ACE constraints, using the same approach as in case of previously presented POCS-ACE method. Some details will be presented at the end of this subsection.

- 9) Apply the IFFT to obtain the time-domain representation of the previously computed signal:

$$\hat{x} = IFFT(\tilde{X}). \quad (7)$$

- 10) Compute the time-domain clipping difference signal, and its corresponding frequency-domain representation:

$$x_{clip}[n] = \hat{x}[n] - x[n], \quad (8)$$

$$X_{clip} = FFT(x_{clip}). \quad (9)$$

- 11) For each sample, compute the projection value according with the following relation:

$$k_{proj}[n] = \Re(x[n] \cdot x_{clip}^*[n]) / |x[n]|, \quad (10)$$

where  $\Re$  denotes the real part of the given complex number and  $x_{clip}^*$  represents the complex conjugate replica of the previously computed clipping delta signal  $x_{clip}$ .

- 12) Compute the approximate balancing for all samples which indicates an amplitude growth, ( $k_{proj} > 0$ ). This can be calculated using one of the following equations:

$$u[n] = \frac{x_{max} - |x[n]|}{k_{proj}[n] - k_{proj}[n_{max}]}, \quad (11)$$

$$u[n] = \frac{x_{max} - |x[n]|}{|x_{clip}[n]| + |x_{clip}[n_{max}]}. \quad (12)$$

Optionally, when a minimum average signal level  $x_{lim}$  is desired, the approximate balancing parameter can be calculated with:

$$u[n] = \frac{x_{max} - x_{lim}}{|x_{clip}[n_{max}]}. \quad (13)$$

This adaptation can be done, when the given minimum threshold fulfills the following condition:

$$x_{max} - u[n] \cdot x_{clip}[n_{max}] < x_{lim}. \quad (14)$$

Details about some these aspects and related practical exemplification are available in the original work [15].

- 13) Normalize the obtained approximate balancing vector, to the unitary range:

$$w[n] = u[n] / u_{max}, \quad (15)$$

where:

$$u_{max} = \max(u[n]). \quad (16)$$

This step was additionally introduced in the algorithm, used in this work, in order to reduce the dynamics of this parameter.

- 14) Compute the new limited time-domain signal, based on the clipped signal and the minimum approximate balancing values, according with the following relation:

$$\tilde{x}_{sgp}[n] = x[n] + w_{min} \cdot x_{clip}[n], \quad (17)$$

where:

$$w_{min} = \min(w[n]). \quad (18)$$

- 15) Repeat the procedure according with the given number of cycles, considering the previously obtained time-domain signal as input data for the presented algorithm.

After some iterations, the PAPR reduction per cycles decreases considerably, therefore, optionally, the practical implementation of this algorithm can be optimized in order to reduce the number of iterations. The break condition is given by the value of the approximate balancing parameter. This criteria and relate practical aspects are also detailed in the original work [15].

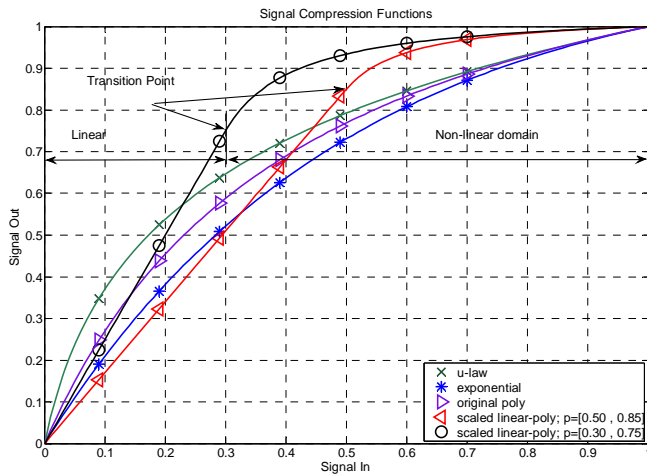


Figure 4. Examples of quasi-nonlinear companding functions.

The presented algorithm performs a gradual projection using a part of the clipping difference at each ACE iteration. The clipping delta signal is obtained by imposing each time the desired threshold to the time-domain signal.

The new proposed CGP-ACE method, instead of using a part of the clipping difference according with a computed ratio at each iteration, applies a progressive signal limitation using a given function. Therefore, in this approach, instead of fixed clipping to the predefined threshold, a progressive signal companding is performed.

The method may present different derivatives according with the chosen compression function. However, since no additional signal distortion or processing at the receiver is desired, the applied compression function must contain a linear part for the sub-domain corresponding to the signal level under the clipping threshold.

In order to realize such transfer function, a quasi-nonlinear compression function of the form proposed in [6] must be used. That type of functions contains a transition point which defines the border between the linear sub-domain and the non-linear sub-domain. Some examples are represented in Figure 5.

Based on these aspects, the implementation of this ACE method requires the following steps:

- 1) Get an OFDM frame with  $N$  subcarriers, represented by the frequency-domain signal  $X_o$ .
- 2) Compute the corresponding time-domain signal  $x[n]$ , by use of IFFT function.
- 3) Compute the signal's maxima, mean and threshold values  $x_{max}$ ,  $x_{mean}$ ,  $x_{thr}$ , same as in the previous algorithm, but only in the first iteration.
- 4) Define the adjustable signal threshold as an increasing value within the range of  $(x_{max}, x_{thr})$ . The present work considers a linear increasing value of the form:

$$x_{adj} = \frac{R-m}{R+2} \cdot x_{max} + \frac{m}{R+2} \cdot x_{thr}, \quad (19)$$

where  $m$  is the index of the current iteration, and  $R$  is the total number of iterations.

- 5) Establish the transition point for the quasi-nonlinear compression function based on the method proposed in [6]. Considering the previously calculated signal parameters, the threshold point is obtained with the following formulas:

$$\begin{cases} p_x = x_{thr} / x_{max} \\ p_y = x_{thr} / x_{adj} \end{cases} \quad (20)$$

- 6) Compute the companded signal and scale it to the adjustable threshold value, according with the following expression:

$$x_{cmp}[n] = f(x[n]) \cdot \frac{x_{adj}}{x_{max}}, \quad (21)$$

where  $f()$  is the quasi-nonlinear companding function, expressed as a ratio of polynomials [6].

- 7) Apply the FFT to compute the frequency-domain representation  $X_{cmp}$  of the previously obtained signal.
- 8) Enforce the ACE constraints, same as in the case of previous algorithms.
- 9) Apply the IFFT in order to obtain the time-domain representation  $\hat{x}$  of the previously computed signal.
- 10) Compute the ACE difference signal, to obtain the increasing amplitudes compared to the original signal:

$$x_{delta}[n] = \hat{x}[n] - x[n], \quad (22)$$

- 11) Compute the new limited time-domain signal, based on the ACE clipped signal and a factor, according with the following expression:

$$\tilde{x}_{cgp}[n] = x[n] + w \cdot x_{delta}[n], \quad (23)$$

where  $w$  is an approximation balance factor, which in case of this algorithm can be constant. When this factor is equal with unity, then the current and previous step are optional.

- 12) Repeat the procedure according with the given number of iterations. The number of cycles can be reduced when the maxim value of the ACE delta signal is smaller than a given value.

This new algorithm performs a gradual projection using as variable characteristic the signal companding function. This function may have different nonlinear characteristics, the main condition being to have a transition point where the linearity of the function changes.

The main common operation of all ACE algorithms is the application of the ACE constraints on the vectors according with the considered extended constellation.

In order to apply the ACE constraints for the outer points of the constellation, their corresponding vectors must be changed. Depending on their relative location versus the location of the original point and on the allowed extended

domain, the algorithm may change vector's amplitude or phase or both.

A solution would be to rotate the vector until the outer point enters back into corresponding extended domain. When this operation is not enough, the vector's amplitude can be increased accordingly.

In the present work, in order to reduce the computation complexity, the ACE constraints are applied by checking and changing the Cartesian coordinates separately. The present algorithm considers: the constellation's minimum-distance  $d_{min}$ , the distance between two adjacent extended domains  $d_{spa}$ , the coordinate of the original outer point and the coordinate of the actual point obtained after clipping. When the in-phase or quadrature value is under the threshold indicated by the corresponding domain border, the difference  $d_{ext}$  is added to shift the point back into its domain. This approach is presented in Figure 5.

Another variant is represented by the particular case where the distance between two adjacent extended domains is set to be equal with the constellation's minimum-distance. In this situation, the only allowed shift of the points is toward constellation's outer region, no lateral offset being permitted. This approach is presented in Figure 6.

For the case of the M-PSK modulation, the ACE constraint is applied using a similar approach. The difference is that for the M-PSK case, all constellation points can be used to lower the PAPR, and their corresponding extended domains are represented by radial sectors with the angular size of  $2\pi/M$  radians.

With a similar approach, in case of M-PSK modulation, a particular variant for ACE constraints can be defined. In this model, for all points within constellation, the only allowed shift is in the direction given by the original vector, any lateral offsets being restricted.

An important aspect to mention is that the BER performance is strongly impacted by the chosen ACE constraint model. Therefore, a more restrictive constraints set imply a better BER performance.

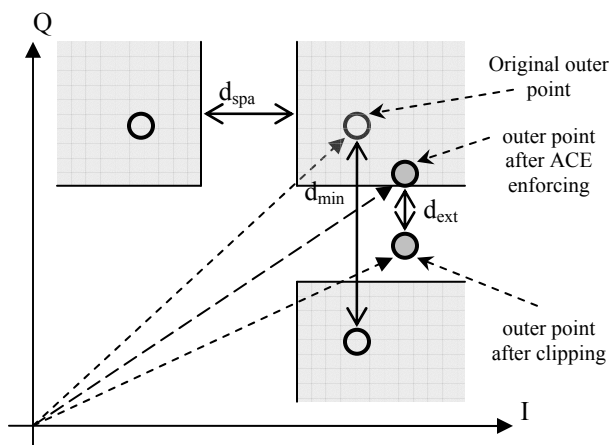


Figure 5. ACE outer point enforcing. Exemplification for 16-QAM.

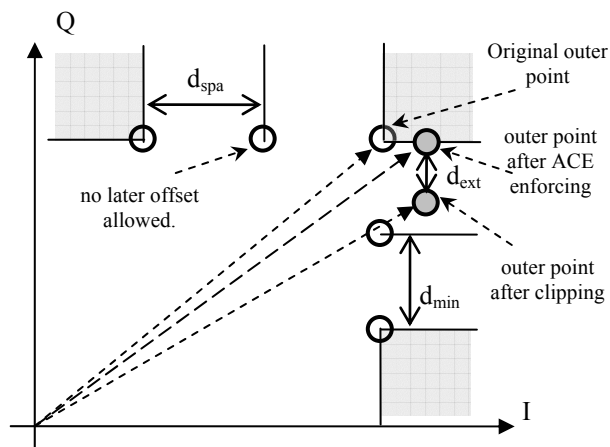


Figure 6. Particular case of ACE outer point enforcing.

### B. The TR method

The TR method performs a frequency-domain adaptation of a given OFDM frame, in order to achieve a lower PAPR level for the corresponding time-domain representation. The changes are applied on the set of non-data carriers. The method performs an iterative search using different combination of complex values from a given set, for the considered subcarriers.

A search for the combination which gives the minimum PAPR level would require an exhaustive amount of operations, due to checking of whole search space of all possible values on all non-data subcarriers. Therefore in most of the cases the algorithm is implemented to search for a suboptimal solution, within a given subspace.

In the previous work [1], the considered TR method, performs a sequential search according with an one-by-one scheme as proposed by [9][14]. The block diagram for this method is presented in Figure 7.

It selects  $T$  pilot tones positions from a complete set of  $Q$  no-data carrier positions and a set of  $M$  complex values, forming a set of  $M^T$  possible combinations.

This search space may lead to an increased amount of computation. The chosen tone reservation algorithm decreases the computation complexity by attempting a reduced search space by trying all  $M$  values on the first pilot  $P[0]$ , while the other pilots,  $P[1], \dots, P[T-1]$ , have a "randomized" or zero initial state. Once an optimal value is found, a similar procedure is repeated on the other pilot positions. For further computation complexity reduction, the time-domain signals equivalent for all pilot tones can be computed and stored initially into memory. In this case, more operations are done in time-domain, fact which determines a decreased number of FFT operations [9].

Because the TR method operates on some subcarriers from the frequency-domain signal, the displacement of these non-data subcarriers may impact the method's performance. Depending by position, the allocation of the reserved subcarriers may be symmetrical or lateral occupying the lower or higher part of the signal's spectrum. The

considered variants are presented in Figure 8, Figure 9, and Figure 10, respectively.

The TR method already presented, may provide a small PAPR reduction, due to the use of a limited search subspace. In order to improve the PAPR reduction, the search subspace can be extended by increasing the set of possible values for each subcarrier. Such approach may provide some PAPR reduction with the cost of considerable increased number of operations. Another extension of the search subspace consists in the increasing of the number of combinations of the considered values.

In the present work, some new sequential TR derivate methods are considered. Within the new proposed SBG-TR derivate method, the considered search subspace is extended with more combinations of the given set of carriers values. For this purpose, the SBG-TR method split the set of non-data subcarriers in groups according with a given pattern. An example of such TR grouping is presented in Figure 11. Each of these groups is considered to be a full search subspace.

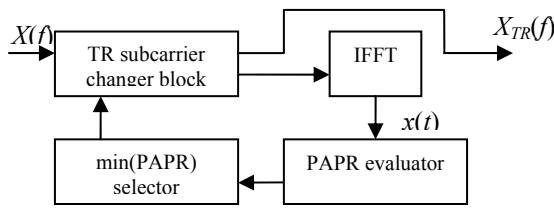


Figure 7. Sequential Tone Reservation method.

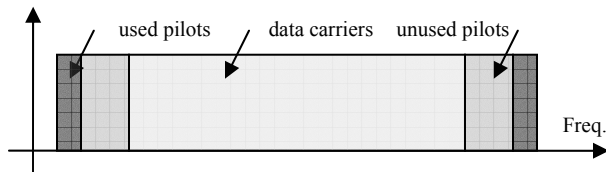


Figure 8. Allocation of reserved tones within an OFDM symbol (symmetrical, outer) Type I

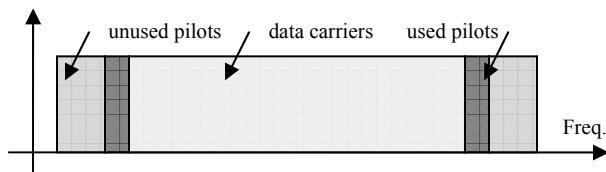


Figure 9. Allocation of reserved tones within an OFDM symbol. (symmetrical, inner) – Type II

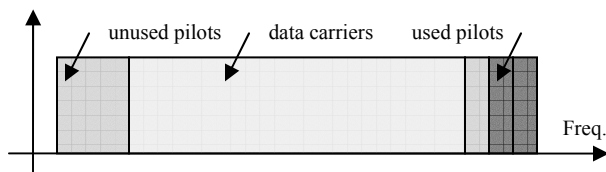


Figure 10. Allocation of reserved tones within an OFDM symbol (lateral, outer) – Type III

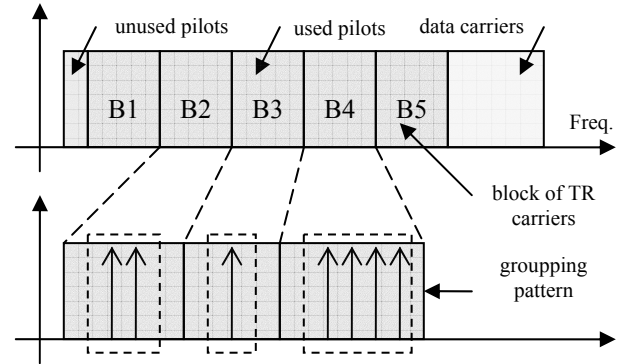


Figure 11. Grouping of TR subcarriers in blocks.

The proposed SBG-TR method, performs search of the optimal combination of vectors values which presents the lowest PAPR within each block, one-by-one. Once the vector values for a block are established, they remain fixed, the search being continued on the next block of non-data subcarriers.

Based on these aspects, the SBG-TR algorithm can be described by the following steps:

- 1) Get an OFDM frame with  $N$  data subcarriers,  $Q$  non-data subcarriers,  $T$  of them being used within the search algorithm.
- 2) Consider a set of  $M$  possible complex values for each vector within the selected  $T$  non-data subcarriers. In a generalized case, this set may be different for each subcarrier. However, for simplicity, in present work it is considered to be identical for each of these subcarriers.
- 3) Based on a given pattern, group the selected TR subcarriers in  $B$  blocks, the number of elements within each block being  $K[j]$ , where  $j=1...B$ .
- 4) Reset all non-data subcarriers to an initial state, composed by zero values.
- 5) For each of the  $B$  blocks, try all  $M^{K[j]}$  combinations, the one presenting the smallest PAPR level for the equivalent time-domain signal representation being stored.
- 6) Optionally, the algorithm may be repeated for another grouping pattern.

The algorithm can be generalized, by considering different order for the TR blocks. The sequence of the block may be ascending, descending, or according with other patterns. Another possible extension of the presented algorithm may consider non-contiguous blocks. These approaches may be used to mix the TR subcarriers from the low frequency domain with those from the high frequency domain.

According with the approach used in this method, the extension of the search subspace is distributed along different parts from the set of TR subcarriers. The size of the search subspace extends with the increase of the number of subcarriers per block. A grouping pattern with fewer subcarriers per block reduces the search subspace accordingly. The particular case of one TR subcarrier per block reduces this algorithm to the original sequential TR method.

Another approach for applying a distributed extension of the search sub-space is to consider a conditioned backtracking algorithm. In this case the total number of backward steps is limited to a given threshold. The forward steps are done when the local gain for PAPR reduction is higher than a given threshold, too. The algorithm may be applied to entire set of TR subcarriers at once, or can be performed on subsets, as in case of the presented algorithm.

When the TR block follows after the ACE block, as Figure 1 indicates, the interfacing of these blocks has to be properly adapted.

Both PAPR reduction blocks have to operate on the same signal, in order to have same frequency spectrum, the non-data subcarriers used within TR block has to be available at the ACE block's input.

The ACE block performs a nonlinear signal processing, which will affect the non-data subcarriers as well. Because these subcarriers are not carrying any information, they have no ACE constraints as method requires for the constellation points of the data subcarriers. From the ACE perspective these non-data subcarriers have the optimal value for lowering PAPR.

Contrary, the TR block will change the values of these non-data subcarriers in order to search an OFDM alternative signal with a decreased PAPR. Because some of these subcarriers will provide no improvement from the PAPR reduction point of view, the initial value set of the ACE block has to be considered.

In order to make the proper adaptation, the TR constellation point set of each non-data subcarrier has to include the initial value obtained after previous signal processing performed by the ACE block.

### III. THE CLIPPING METHOD

For analysis of the efficiency of the proposed hybrid technique, also a pure nonlinear method has been considered. This is the clipping method with frequency-domain filtering as presented in [18]. The block diagram of this method is presented in Figure 12. It consists in a zero padding block, an IFFT block, an effective clipping block, and a frequency domain block. For a frequency-domain input signal represented by a vector  $A_{in}$  with  $N$  elements  $[a_0, \dots, a_{N-1}]$  and an oversampling factor  $p$ , the zero padding inserts  $N(p-1)$  zeros in the middle of this vector, forming the new vector  $A_{zp}$ . The clipping block limits the amplitude of the time-domain signal to a given threshold. The resulted signal  $a_{clip}$  is then applied to the frequency domain filter where the output signal  $a_{out}$  is obtained.

The clipping ratio ( $CR$ ) applied in this method is defined as ratio of the clipping level  $A$  to the root-mean-square power  $\sigma$  of the unclipped baseband signal, being described by the following expression:

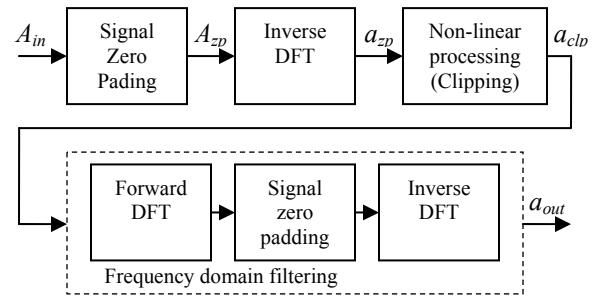


Figure 12. Clipping with filtering PAPR reduction method.

$$CR = 20 \cdot \log_{10} \left( \frac{A}{\sigma} \right). \quad (24)$$

The filtering block is composed by an FFT block, another zero padding block and an IFFT block. It is designated to reduce the out-of-band noise without distorting the in-band discrete signal.

### IV. SIMULATION RESULTS

The MATLAB simulations have been performed for base-band signals with  $N=128$  subcarriers using M-QAM and M-PSK modulations. The frequency-domain signal is extended with additional  $Q=24$  no-data subcarriers. From this set,  $T=12$  subcarriers are used for PAPR reduction by the TR method. The corresponding constellation consists in sets of  $M=16$  points. For the reference clipping method, the simulation considers the clipping rate  $CR$  having some values in the range of 6-14 and the oversampling factor  $p$  set to 2.

For the OFDM signal spectrum computation, it was considered that the distance between two adjacent subcarriers is 0.2 MHz.

The results presented in this paper are obtained for OFDM frames with the repartition of non-data subcarriers as previously indicated in Figure 8, Figure 9, and Figure 10, with constellations of the pilot search space points identically with the constellations of the constellation used for data carriers.

These results consider various combinations of the POCS, SGP and CGP ACE methods with the sequential and SBG TR method.

The simulation results show that the proposed scheme improves the PAPR reduction in comparison with the use of only one of the component methods. The improvement for the case of POCS-ACE with sequential TR methods is highlighted in this section with three cases.

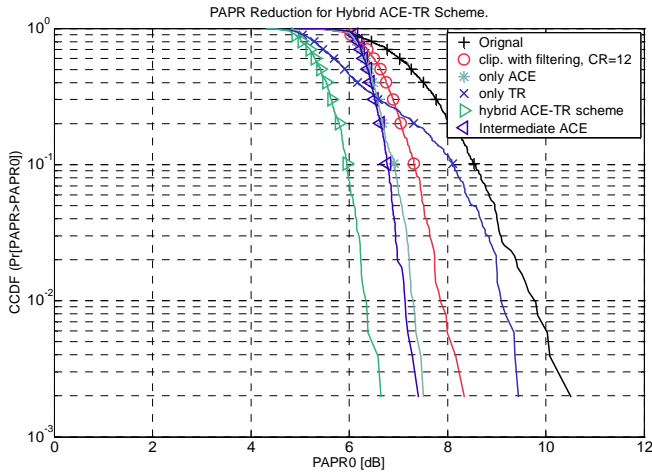


Figure 13. PAPR reduction using hybrid POCS ACE-TR method. Type I

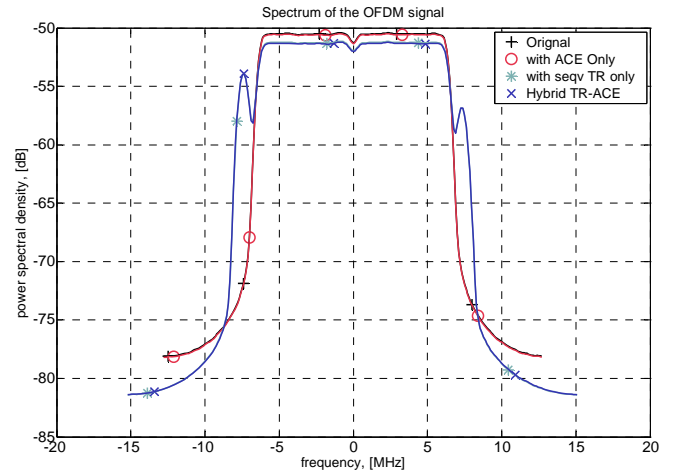


Figure 16. PSD of OFDM signal before/after PAPR reduction. Type I

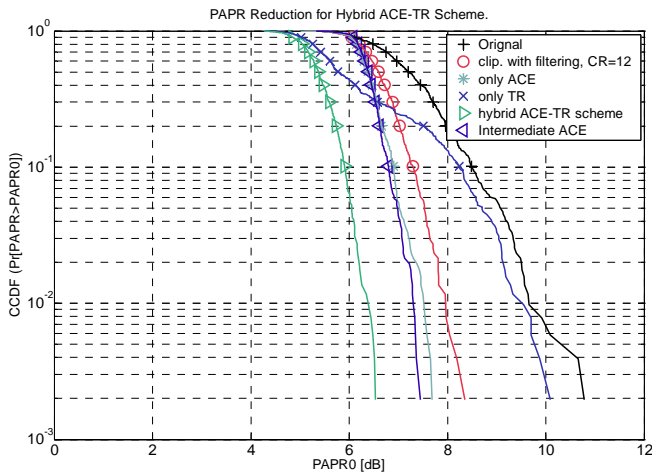


Figure 14. PAPR reduction using hybrid POCS ACE-TR method. Type II

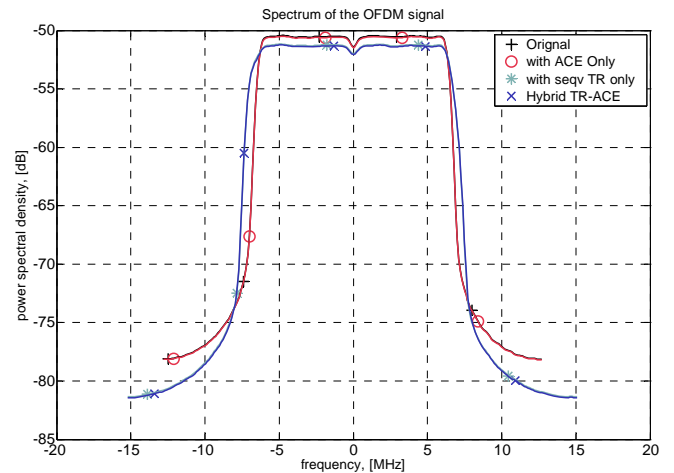


Figure 17. PSD of OFDM signal before/after PAPR reduction. Type II

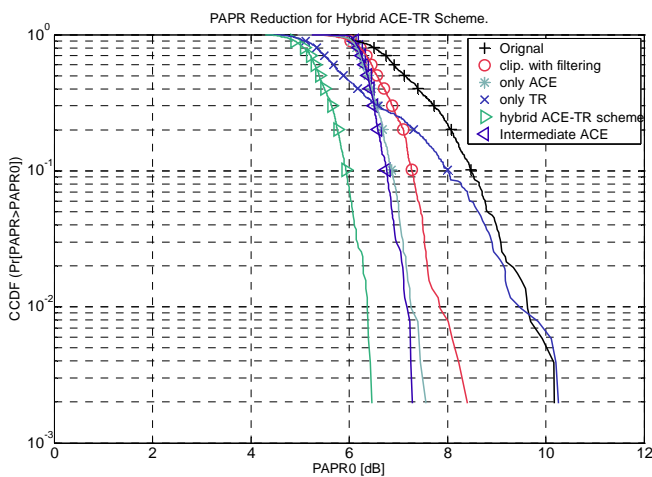


Figure 15. PAPR reduction using hybrid POCS ACE-TR method. Type III

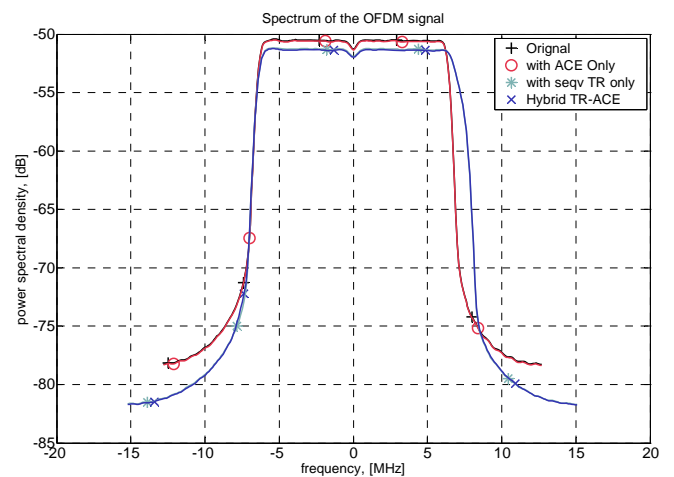


Figure 18. PSD of OFDM signal before/after PAPR reduction. Type III

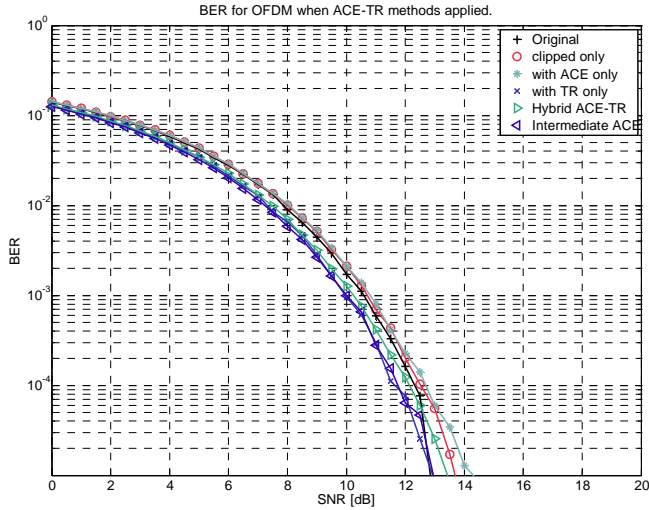


Figure 19. BER of OFDM signal before and after PAPR reduction.

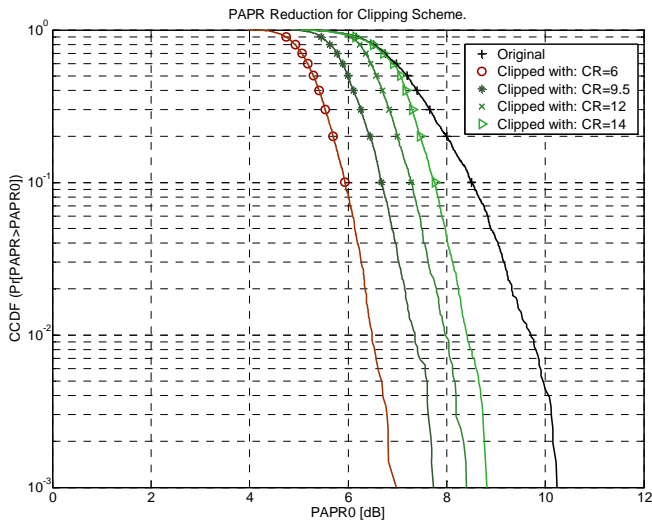


Figure 20. PAPR reduction using clipping method.

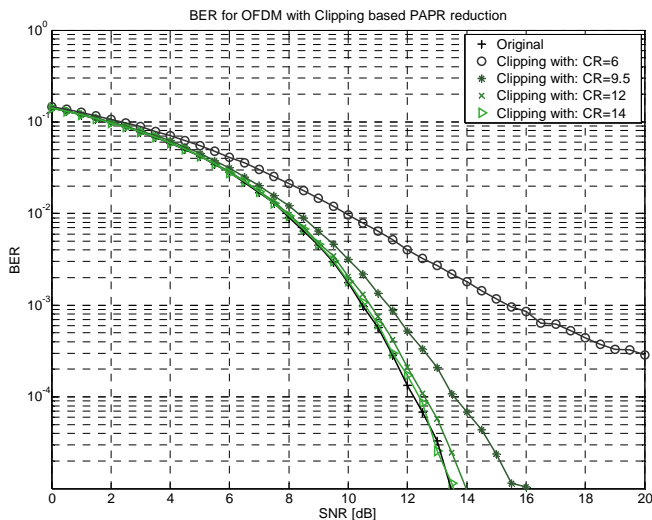


Figure 21. BER of OFDM signal before/after clipping.

In the first case, Figure 13 and Figure 16 indicate the PAPR reduction and signal's frequency spectrum when the OFDM frame has the non-data subcarriers configuration as presented in Figure 8.

In Figure 13, it can be observed that the ACE method performs a better PAPR reduction while the applied TR method obtains a lower PAPR reduction than the clipping at a ratio of  $CR=12$ . A slight difference can be observed between the ACE applied on the initial OFDM frame and the extended OFDM frame containing the reserved non-data subcarriers. The hybrid ACE-TR provides better PAPR reduction since it accumulates the effects from the two methods.

Due to the insertion of the additional non-data subcarriers on the both sides of the original spectrum, the obtained signal presents an increased bandwidth as indicated in Figure 16.

In the second case, Figure 14 and Figure 17 indicate the PAPR reduction and signal's frequency spectrum for the configuration shown in Figure 9.

Due to a different displacement of the non-data subcarriers, the TR method has a different efficiency for the PAPR reduction. Even if this method has smaller PAPR reduction, with the hybrid method still higher PAPR reduction is obtained. Also, this case presents a smaller increase of the bandwidth for the resulted OFDM signal than the one from the previous one.

In the third case, similarly, Figure 15 and Figure 18 indicate the same signal parameters when the non-data subcarriers are located as is shown in Figure 10.

For the PAPR reduction, this case is quite similar with the first one. The difference consists on the spectrum of the resulted signal, which has a slightly asymmetrical shape.

Figure 19 shows that the BER performance is slightly influenced by the proposed PAPR reduction technique, being better than in case of simple clipping.

For a better evaluation of the performance of the proposed method, the PAPR reduction and corresponding BER characteristic of the clipping method are presented in Figure 20 and Figure 21, respectively.

The simulations shown that, if smaller values for the clipping ratio are considered, the clipping method obtains comparable PAPR reduction as the hybrid method do. The drawback of this case is that the smaller  $CR$  values imply an increased signal distortion, and so a worst BER performance.

Therefore the presented simulation results shown that, in all these cases, the hybrid ACE-TR method provides better PAPR reduction than in case of use of only one component method. Additionally, compared with clipping, the combined technique presents no degradation of the BER performance.

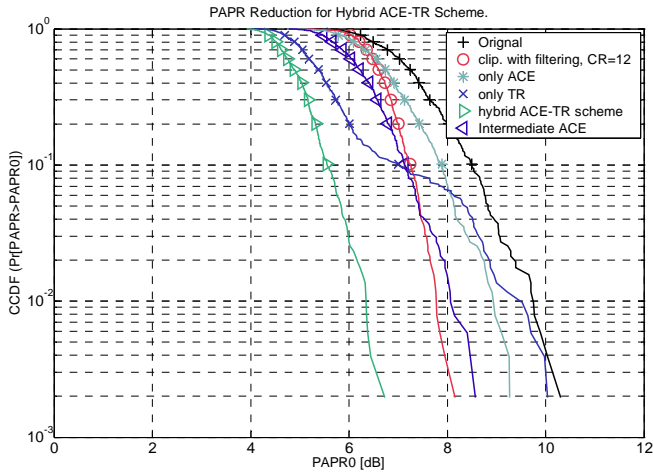


Figure 22. PAPR reduction using hybrid SGP ACE-TR method. Type I

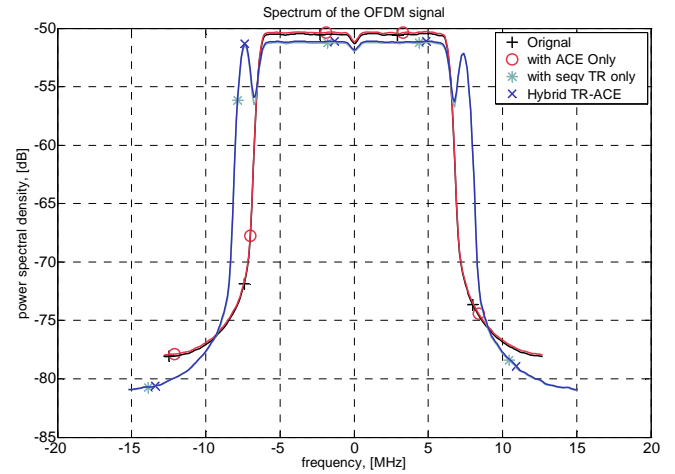


Figure 25. PSD of OFDM signal before/after PAPR reduction. Type I

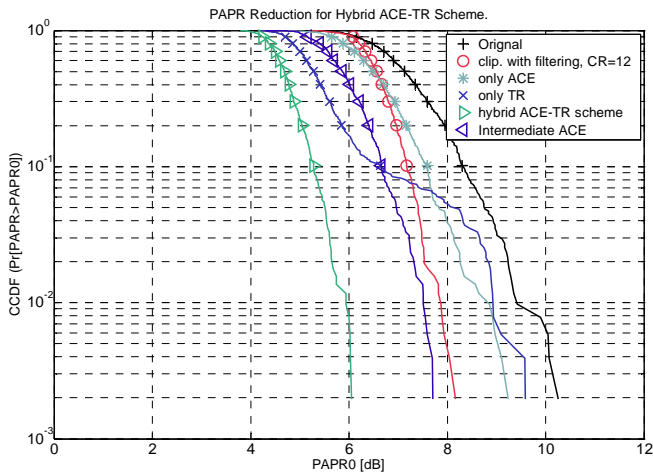


Figure 23. PAPR reduction using hybrid SGP ACE-TR method. Type II

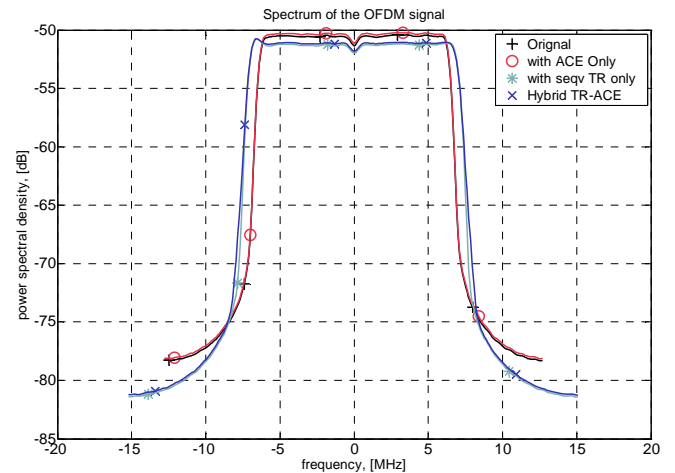


Figure 26. PSD of OFDM signal before/after PAPR reduction. Type II

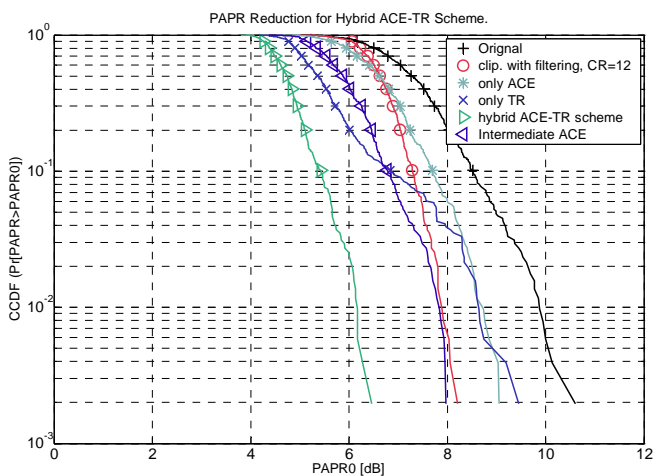


Figure 24. PAPR reduction using hybrid SGP ACE-TR method. Type III

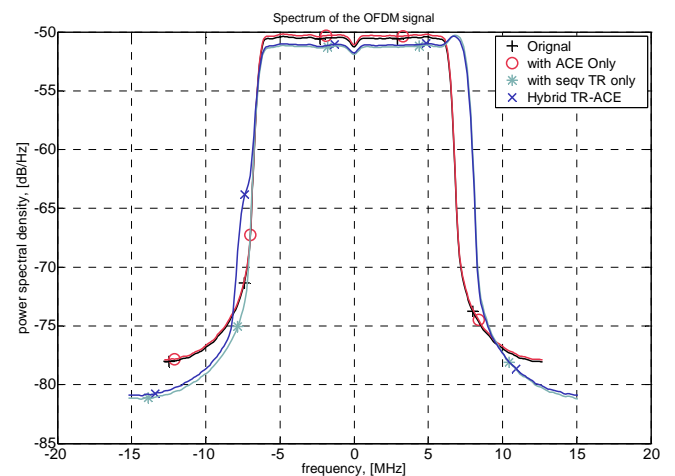


Figure 27. PSD of OFDM signal before/after PAPR reduction. Type III

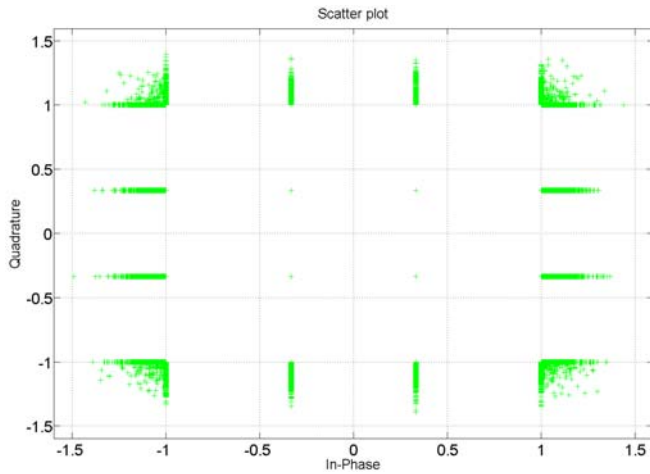


Figure 28. Constellation points dispersion plot in case of hybrid SGP ACE-SBG TR method.

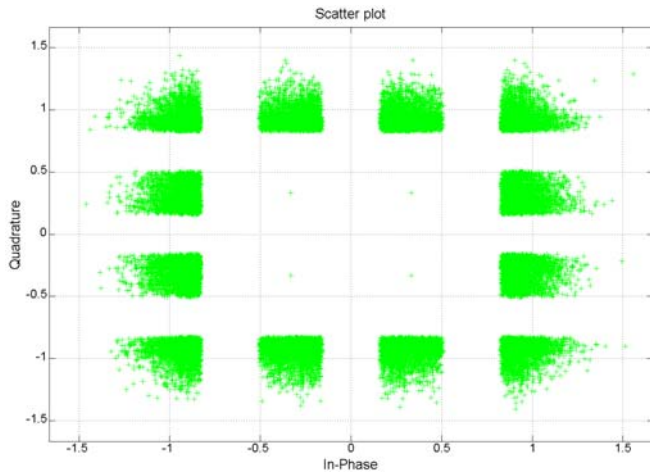


Figure 29. Constellation points dispersion plot in case of hybrid SGP ACE-SBG TR method.

Similar results are obtained when the hybrid scheme uses the SGP ACE and sequential block grouped TR methods. The simulation results are presented for the same non-data subcarrier displacements as presented before.

The used SGP ACE method is based on the approaching balancing according to relation (11) and is set to use 4 iterations per OFDM frame. The sequential block grouping TR method is configured to use 3 subcarriers per block.

The PAPR reduction and signal's frequency spectrum for the first case are presented in Figure 22 and Figure 25 respectively.

Compared with the previous situation, the ACE presents a similar performance like the clipping method. The difference is due to a stronger ACE constraint for constellation points, as presented in Figure 28. The TR schemes also provide a slight different result due simultaneous check of more TR subcarriers.

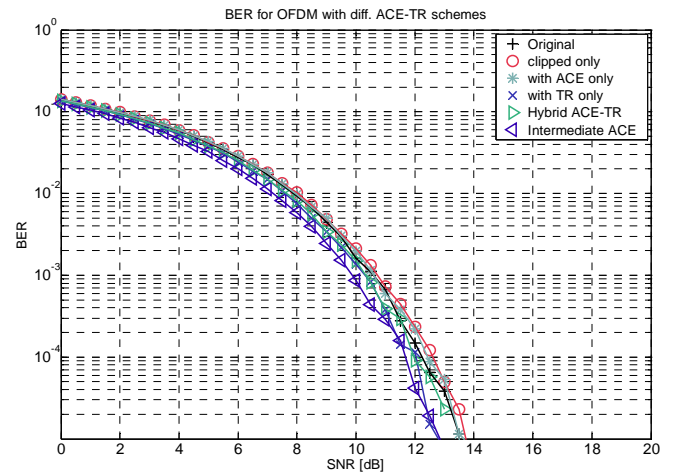


Figure 30. BER of OFDM signal before and after PAPR reduction in case of strength constellation condition.

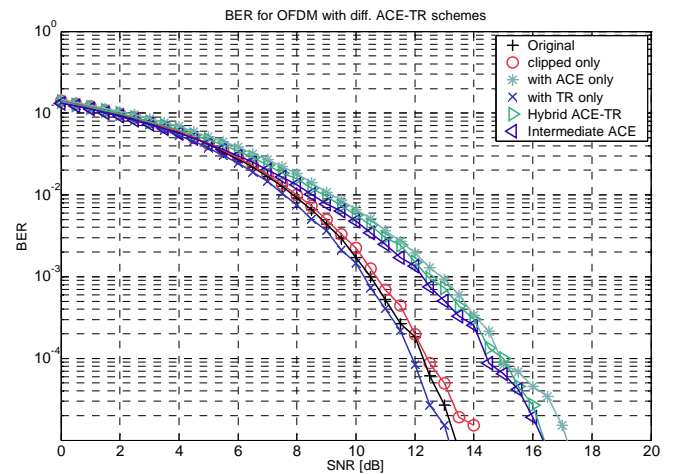


Figure 31. BER of OFDM signal before and after PAPR reduction in case of relaxed constellation condition.

The results for the second case, presented in Figure 23 and Figure 26 respectively, have the same characteristics. Compared with the previous hybrid scheme, in this case the ACE and TR performances are different, the PAPR reduction efficiency of a method being compensated by the other one.

The results for the third case are presented in Figure 24 and Figure 27 respectively. The good efficiency of the SBG TR method is reflected also in the spectral characteristic, where appearance of some non-data subcarriers is observable by the wider bandwidth.

The BER performance corresponding to these cases is shown in Figure 30.

When the ACE constraints become less restrictive, as presented in Figure 29, the PAPR reduction efficiency increases. The disadvantage in this situation is the higher BER degradation as presented in Figure 31.

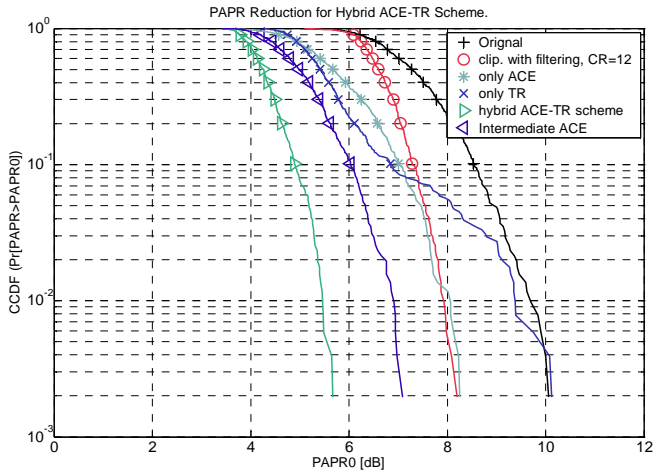


Figure 32. PAPR reduction using hybrid SGP ACE-TR method. Type I

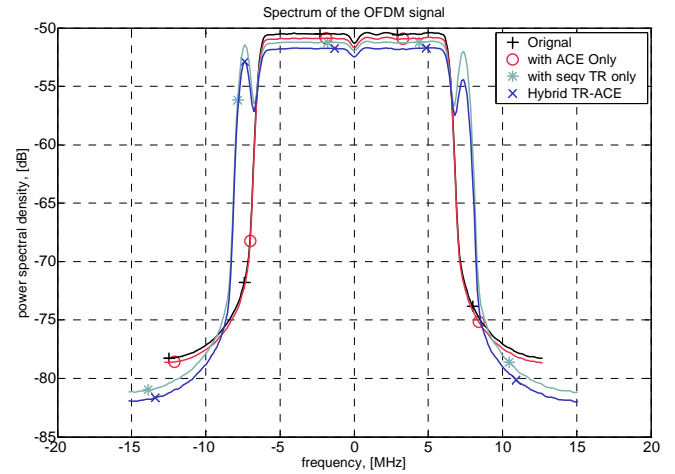


Figure 35. PSD of OFDM signal before/after PAPR reduction. Type I

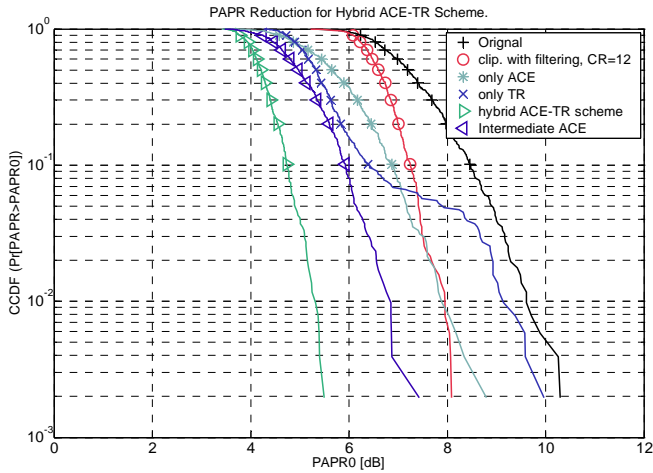


Figure 33. PAPR reduction using hybrid SGP ACE-TR method. Type II

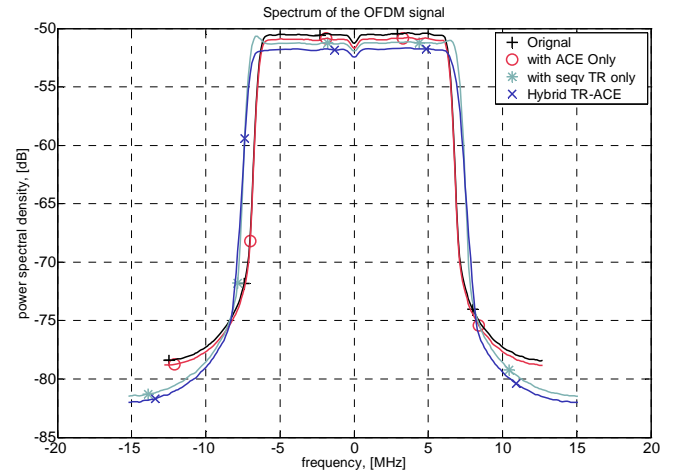


Figure 36. Spectr. of OFDM signal before/after PAPR reduction. Type II

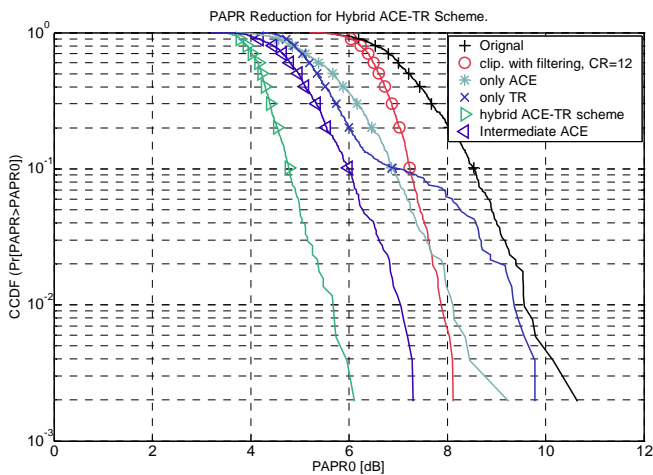


Figure 34. PAPR reduction using hybrid SGP ACE-TR method. Type III

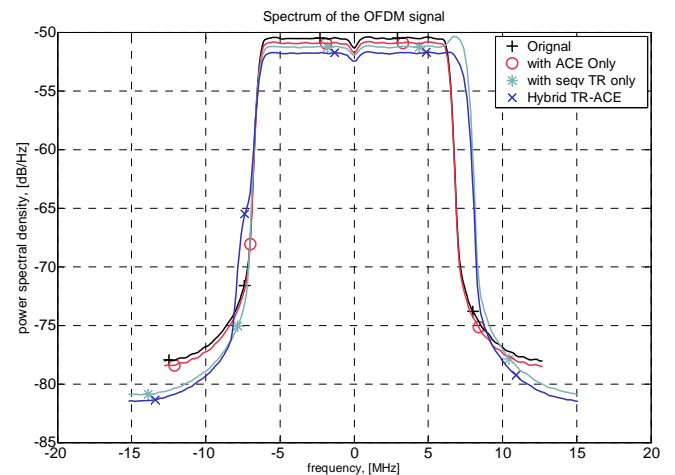


Figure 37. PSD of OFDM signal before/after PAPR reduction. Type III

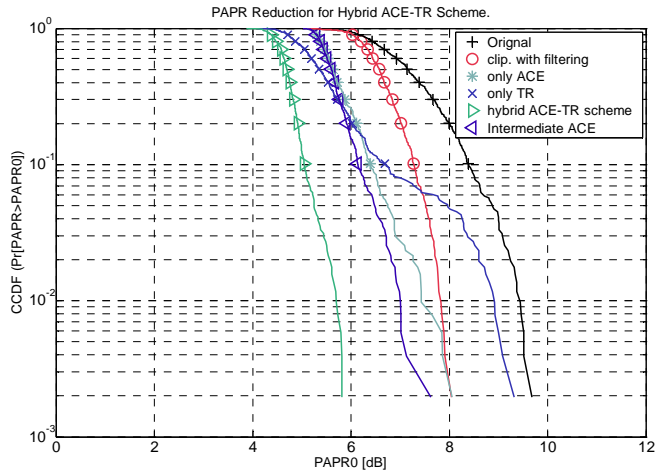


Figure 38. PAPR reduction using hybrid CGP ACE-TR method. Type I

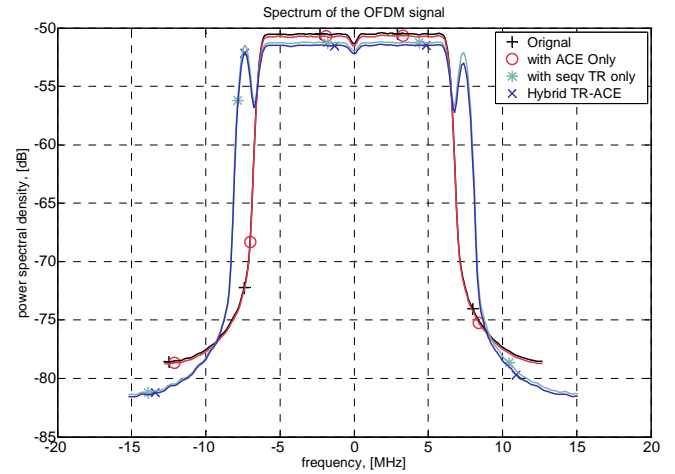


Figure 41. PSD of OFDM signal before/after PAPR reduction. Type I

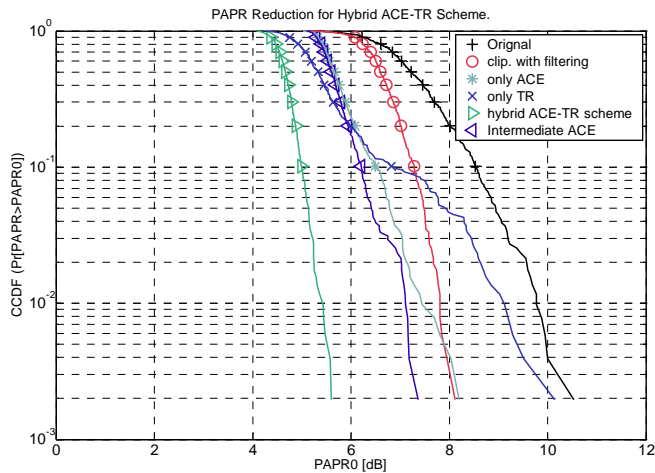


Figure 39. PAPR reduction using hybrid CGP ACE-TR method. Type II

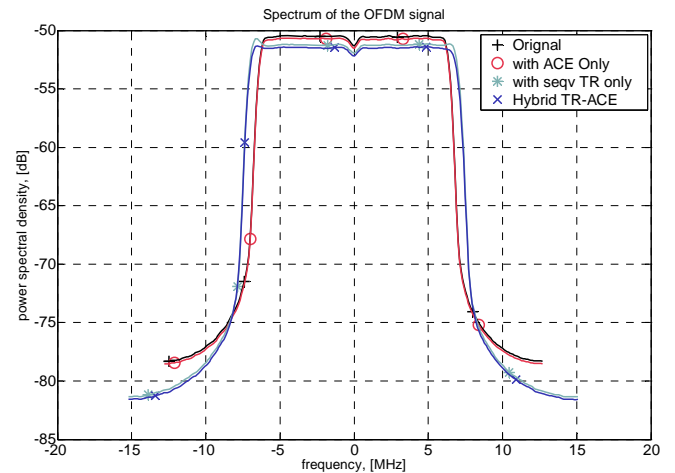


Figure 42. PSD of OFDM signal before/after PAPR reduction. Type II

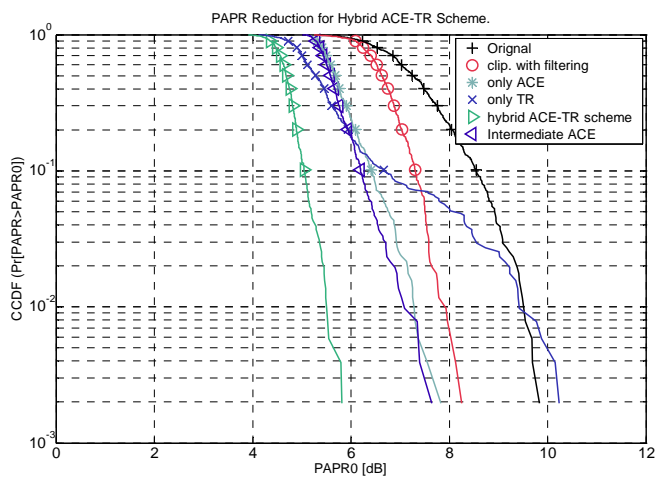


Figure 40. PAPR reduction using hybrid CGP ACE-TR method. Type III

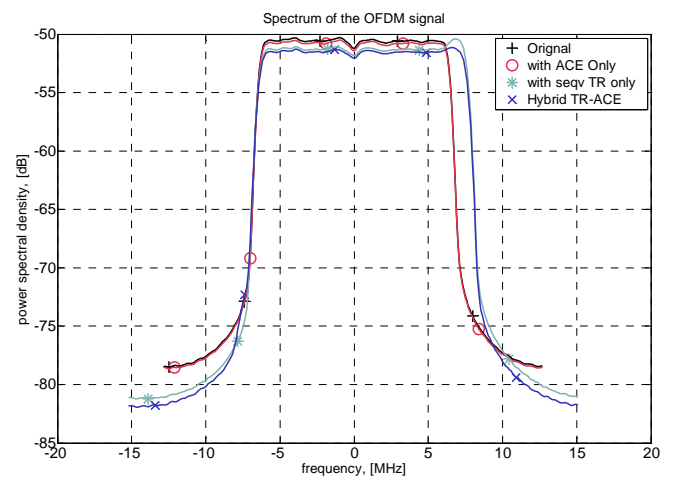


Figure 43. PSD of OFDM signal before/after PAPR reduction. Type III

The simulation results shown that for this relaxed constellation constraints, ACE component method provides better PAPR reduction efficiency.

The simulation results for PAPR reduction and spectral characteristic for the case with the non-data subcarriers displacement of type I, using the SBG ACE method are presented in Figure 32 and Figure 35, respectively. In this case the ACE method presents a better PAPR reduction efficiency compared with the referenced clipping, having a slight BER performance degradation.

Similar simulation results for PAPR reduction and spectral characteristic for the case with non-data subcarriers displacement of type II are presented in Figure 33 and Figure 36, respectively.

The next case, when the non-data subcarriers displacement of type III is used, is presented in Figure 34 and Figure 37, respectively.

A specific aspect of these cases is the slightly different maximal spectral amplitude. This is caused by the different results of the TR method due to the relaxed ACE constraints.

The simulations results consider the new CGP-ACE derivate method as well. For this scheme, the simulations consider 4 iterations, with a fixed step size of 0.7 for the clipping delta signal.

The corresponding PAPR reduction and signal's frequency spectrum for the considered repartition for the non-data subcarrier are presented in the next diagrams as followings: Figure 38 and Figure 41 for the type I, Figure 39 and Figure 42 for the type II and Figure 40 and Figure 43 for type III, respectively.

The simulation results show that the CGP-ACE method presents similar PAPR reduction performance as the SGP-ACE method. Due to its different approach, the time-domain samples have another statistical distribution. The corresponding frequency-domain signal changes accordingly, therefore a slightly different PAPR reduction of the TR method will be obtained.

Therefore, the presented simulation results show that the hybrid method presents a better PAPR reduction also when the SGP ACE and CGP ACE are considered. The new SBG TR method presents a different performance, which is strongly dependent by the used block grouping pattern.

The BER performance depends by the ACE constraints applied on each iteration.

The computational complexity of the algorithm of the hybrid technique is given by the sum of the computational complexity of the component methods. The total amount of operations depends by the used ACE and TR derivate methods.

In case of POCS method, the ACE block performs one IFFT, one clipping, one FFT and one vector shift per iteration. For the presented simulations, we have limited the number of iterations in the ACE block to one, therefore the amount of operations for this block is  $O(2 + 2 \cdot N \cdot \log_2(N))$ .

In case of the SGP ACE and CGP-ACE, the number of operations increases due to the computing of the approximate balancing factor and signal companding. Therefore the amount of operations for these ACE blocks is of  $O(C \cdot (B + 2 \cdot N \cdot \log_2(N)))$ , where  $C$  is the number of cycles, and  $B$  is the number of operations needed to compute approximate balancing factor or companded signal. For the considered SGP and CGP ACE methods, the additional amount of operations  $B$  can be approximated to  $4 \cdot N$ .

In case of the sequential TR method, the PAPR reduction block performs one change for a pilot subcarrier and one IFFT per iteration. Considering the applied algorithm and the size of the search space, a complete operation requires  $O(M \cdot T \cdot (1 + N \cdot \log_2(N)))$  computations.

In practice, the amount of operations can be reduced if the time-domain signal corresponding to each single non-data subcarrier is pre-computed and stored in a nonvolatile memory. In this case the amount of operations is reduced to  $O(M \cdot T + N \cdot \log_2(N))$ .

In case of the sequential block grouping TR method, where for each block, all possible combinations are evaluated, and the total amount of operations increases. When the method uses  $B$  blocks, the number of carriers per block is  $K = T / B$ , therefore the total amount of operations is:  $O(B \cdot M^K \cdot (1 + N \cdot \log_2(N)))$ .

Based on these expressions, it can be observed that the amount of operations required by the hybrid method is bigger than the number of operations required by other PAPR reduction techniques and depends by number of data subcarriers and the size of the search space used by the TR block.

## V. CONCLUSION AND FUTURE WORK

In this paper, which represents a development of [1], we proposed a new PAPR reduction technique based on the combination of different active constellation extension methods with different tone reservation methods.

The paper presents the ACE and TR algorithms used within the hybrid technique. The interfacing of the two PAPR reduction blocks is also explained. Besides the well known POCS and SGP ACE derivatives, the new CGP ACE was proposed. Also for the TR technique, the new SBG-TR derivate method was proposed. These new PAPR reduction methods permit the development of the analysis presented in the original work.

The simulation results, which enhance the results reported in original work, show that the hybrid scheme realizes higher PAPR reduction for various OFDM frame formats. Similar results for PAPR reduction have been obtained for the case when TR block precedes the ACE block.

The ACE and TR methods have various derivatives, bringing different efficiency and performance. The ACE method may be implemented using different constellation restrictions, obtaining different PAPR reduction levels and BER performances. The TR method may use different set of values for the non-data subcarriers. Depending on this set, its computation complexity and PAPR reduction strength may

significantly vary. In case of the proposed SBG TR method, the performance depends by the used block grouping pattern and pilot subcarrier displacement, too.

Compared with other PAPR reduction methods like SLM and PTS, the ACE and TR methods presents a variable PAPR reduction efficiency depending by selected parameters. In many cases their PAPR reduction gain decreases after several iterations.

Therefore the SLM and PTS methods may present increased PAPR reduction, but have the disadvantage of an increased amount of computation complexity due to expended search space.

In future work, we will consider different ACE constraints and TR schemes with different numbers and various sets of values for the non-data carriers.

#### REFERENCES

- [1] V. Cuteanu and A. Isar, "PAPR Reduction of OFDM Signals using Active Constellation Extension and Tone Reservation Hybrid Scheme", The Eight Advanced International Conference on Telecommunications, pp. 156-163, June 2012.
- [2] V. Cuteanu and A. Isar, "PAPR Reduction of OFDM Signals using Partial Transmit Sequence and Clipping Hybrid Scheme", The Eight Advanced International Conference on Telecommunications, pp. 164-171, June 2012.
- [3] V. Cuteanu and A. Isar, "PAPR Reduction of OFDM Signals Using Selective Mapping and Clipping Hybrid Scheme", The 20th European Signal Processing Conference, pp. 2551-2555, August 2012.
- [4] V. Cuteanu and A. Isar, "Hybrid PAPR Reduction Scheme with Selective Mapping and Tone Reservation", International Conference on Applied Electronics, pp. 55-58, September 2012.
- [5] V. Cuteanu and A. Isar, "PAPR reduction of OFDM signals using hybrid clipping-companding scheme with sigmoid functions", International Conference on Applied Electronics, pp. 75-78, September 2011.
- [6] V. Cuteanu and A. Isar, "PAPR Reduction Scheme with Clipping and Quasilinear Sigmoid Compression Functions", International Conference on Applied Electronics, pp. 59-64, September 2012.
- [7] S. Muller, R. Bauml, R. Fischer, and J. Huber, "OFDM with reduced peak-to-average power ratio by multiple signal representation", Annals of Telecommunications, vol. 53, pp. 58-67, February 1997.
- [8] L. J. Cimini Jr. and N. R. Sollenberger, "Peak-to-average power ratio reduction of an OFDM signal using partial transmit sequences", IEEE Commun. Lett., vol. 4, no. 3, pp. 86-88, March 2000.
- [9] Y.Z. Jiao, X.J. Liu, and X.A. Wang, "A Novel Tone Reservation Scheme with Fast Convergence for PAPR Reduction in OFDM Systems", Consumer Communications and Networking Conference, pp. 398-402, January 2008.
- [10] L. Wang and Y. Cao, "Improved SLM for PAPR Reduction in OFDM Systems", International Workshop on Intelligent Systems and Applications, pp. 1-4, May 2009.
- [11] L. Wang and J. Liu, "PAPR Reduction of OFDM Signals by PTS With Grouping and Recursive Phase Weighting Methods", IEEE Transactions on Broadcasting, vol. 57, no. 2, pp. 299-306, June 2011.
- [12] S. Yoo, S. Yoon, S.Y. Kim, and L. Song, "A novel PAPR reduction scheme for OFDM systems: selective mapping of partial tones (SMOPT)", IEEE Transaction on Consumer Electronics, vol. 52, no. 1, pp. 40-43, February 2006.
- [13] E. Bouquet, S. Haese, M. Drissi, C. Moullec, and K. Sayegrih, "An innovative and low complexity PAPR reduction technique for multicarrier systems," Proc. 9th European Conference on Wireless Technology, pp. 162-165, September 2006.
- [14] C. L. Wang, Y. Ouyang, and H. C. Chen, "A low-complexity peak-to-average power ratio reduction technique for OFDM-based systems", Proc. 60th IEEE Vehicular Technology Conference, vol. 6, pp. 4380-4384, September 2004.
- [15] B.S. Krongold and D. L. Jones, "PAPR Reduction in OFDM via Active Constellation Extension", IEEE Transactions on Broadcasting, Vol. 49, No. 3, pp. 258-268, September 2003.
- [16] A. Kliks and H. Bogucka, "Improving Effectiveness of the Active Constellation Extension Method for PAPR Reduction in Generalized Multicarrier Signals", SpringerLink, Wireless Personal Communication, vol. 61, no. 2, pp. 323-334, May 2010.
- [17] M. Malkin, B. Krongold, and J. M. Cioffi, "Optimal constellation distortion for PAPR reduction in OFDM systems", IEEE 19th Int. Symposium on Personal, Indoor and Mobile Radio Communications, pp. 1-5, September 2008.
- [18] J. Armstrong, "New OFDM Peak-to-Average Power Reduction Scheme", Proc. of IEEE Vehicular Technology, pp. 756-760, May 2001.
- [19] M. Deumal, C. Vilella, J. L. Pijoan, and P. Bergada, "Partially Clipping (PC) Method for the Peak-to-Average Power Ratio (PAPR) Reduction in OFDM", IEEE Int. Symposium on Personal, Indoor and Mobile Radio Communications, vol. 1, pp. 464-468, September 2004.
- [20] X. Wang, T. T. Tjhung, C. S. Ng, and A. A. Kassim, "On the SER Analysis of A-Law Companded OFDM System", in Proc. Global Telecommunication Conference, vol. 2, pp. 756-760, December 2000.
- [21] T. Moazzeni, H. Selvaraj, and Y. Jiang, "A Novel Multi-Exponential Function-based Companding Technique for Uniform Signal Compression over Channels with Limited Dynamic Range", Intl. Journal of Electronics and Telecommunications, Vol. 56, No. 2, pp. 125-128, June 2010.
- [22] X. Huang, J. Lu, J. Zheng, and J. Gu, "Piecewise-scales transform for the reduction of PAPR of OFDM signals", IEEE Global Telecommunications Conference, vol. 1, pp. 564-568, November 2002.